Effect of Agglomerated TiO_2 Powders with Nanostructure on Microstructure of Thermal Sprayed TiO_2 coatings †

OHMORI Akira*, NAKADE Katsuyuki**, YASUOKA Junichi*** and NAGAYA Tatsuya***

Abstract

The effect of nanostructure in agglomerated TiO_2 powders on the microstructure and crystal structure of TiO_2 coatings is examined. TiO_2 coatings on SUS304 plate were sprayed by plasma spray and high velocity oxy-fuel (HVOF) spray using two agglomerated TiO_2 powders with nano and sub-micron structures.

The feedstock powders were synthesized via polyvinyl alcohol to produce spherical-shape agglomerates with an average grain size of 30-40μm from the original 200nm and 30nm particles. The powders were then introduced into the plasma and HVOF flame to produce a nanocrystalline coating. For HVOF spray process, various fuel gas pressures were used to find the best parameters. As a result, high anatase ratios could be achieved when HVOF was used at low fuel gas pressure (0.35MPa) by TiO_2 powders with particle sizes of 30nm.

KEY WORDS: (TiO_2 coating) (Plasma spray) (High velocity oxy-fuel (HVOF)) (Anatase TiO_2) (Nano TiO_2 structure)

1. Introduction

TiO_2 is widely applied as a photocatalyst for photodecomposition of polluted water and harmful chemical compounds [1)~5)]. Powders with a large specific surface are promising to fully utilize the photocatalytic property. However, in many case, the powers have to fix on the targeted substrate for practical applications. There have been many reports [6)~7)] about the preparation of thin film TiO_2 coatings such as sol-gel or similar thin film processes. On the other hand, thermal sprayed coatings produce thick layers of lamellar structures with many pores. These pores are very useful as sites for photocatalytic reaction. In addition, thermal sprayed coatings can be easily prepared on many materials such as plastics, metal and ceramics. TiO_2 coating with anatase phase and nano-size structures can drastically improve photocatalytic activity. However, thermal spraying with nano-sized powders is not easy because of the difficulty of powder feeding. And, the problem of easy phase transformation to rutile, which is not helpful for photocatalytic applications, has also to be overcome. In this research, the effect of agglomerated TiO_2 powders with nano- and submicron size primary particles on the microstructure and crystal structure of TiO_2 coatings was investigated by two different processes, namely, plasma spray and high velocity oxy-fuel (HVOF) spray.

2. Experimental Details

2.1 Materials and Characterization

A Cu undercoat was used to increase adhesion strength between topcoat and undercoat. **Fig.1** shows the surface morphology and X-ray diffraction pattern of Cu powders. TiO_2 powders were sprayed after the undercoat to form a topcoat.

Fig.2 shows the surface morphology of two type of TiO_2 powders. P_{200} powders with an average size of 33.7μm were spherical and agglomerated TiO_2 powder, consisting of anatase 200nm particles (ST-41). P_{30} powders were agglomerated TiO_2 powders with an average size of 36.1μm, consisting of anatase 30nm particles (AMT-600). The feedstock powders (200nm and 30nm) were synthesized from polyvinyl alcohol. The polyvinyl alcohol plays the role of binder to produce spherical-shaped agglomerates with average sizes of 30-40μm.

A scanning electron micrograph was used to examine the properties of feedstock powders and sprayed coatings.

X-ray diffraction was employed to confirm the content

† Received on May 31, 2002

* Professor

** Post doctoral research fellow

*** Graduate Student

Transactions of JWRI is published by Joining and Welding Research Institute of Osaka University, Ibaraki, Osaka 567-0047, Japan

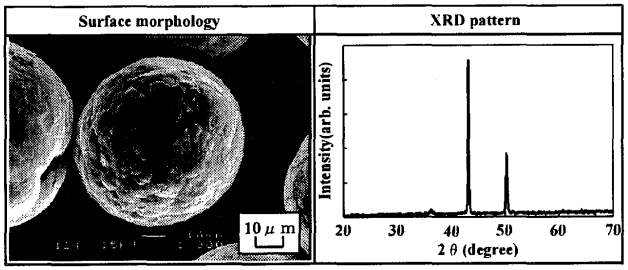

Fig.1 Surface morphology and X-ray diffraction pattern of Cu powders.

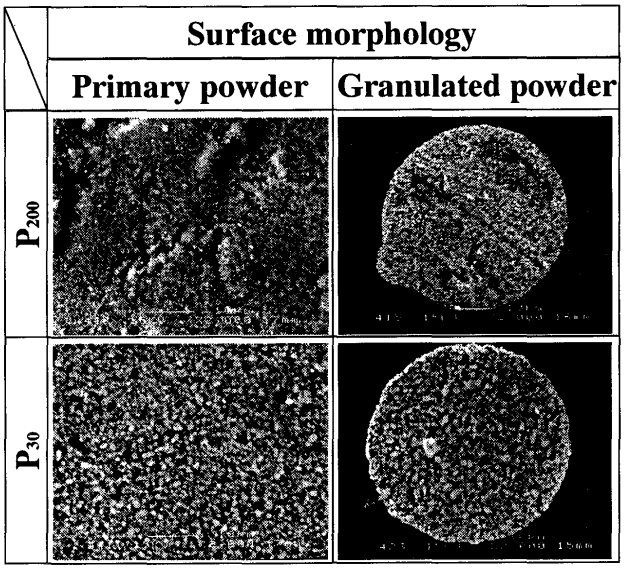

Fig.2 Surface morphologies and particle morphologies of various anatase-TiO_2 powders.

of anatase and rutile phase with K_α radiation and a copper target. From the X-ray diffraction results, the content of anatase TiO_2 in the coating was estimated by the equation (1) [8].

$$f = \frac{1}{1+1.265\frac{I_R}{I_A}} \times 100(\%) \qquad (1).$$

where I_A is the highest peak intensity due to anatase phase , I_R is the highest peak intensity due to rutile phase, f is the content of anatase TiO_2 in the coatings.

2.2 Thermal spray processing

The spraying was carried out using two type of equipment. One was the plasma spraying equipment, whose commercial gun name is Plasma Dyne Gun. Argon was employed as a primary plasma gas and helium as a secondary gas. Spray conditions of the plasma spray are shown in **Table 1**. The powders are carried from the inside of the gun to the plasma jet and finally into the substrate. Particle temperature will increase up to nearly 2000K because the plasma jet temperature becomes 10000 K.

The second equipment was the High Vel ocity Oxygen Fuel (HVOF) apparatus. The fuel gas used was a mixture

Table 1 Spray conditions of plasma spray (plasma dyne).

Ar pressure	0.42(MPa)
He pressure	0.21(MPa)
Arc current	400~800(A)
Arc voltage	28(V)
Spray distance	70(mm)
Traverse speed of gun	8.3×10^{-2} (mm/s)
Step width	4.0mm

Table 2 Spray conditions of HVOF.

O_2 pressure	**0.55(MPa)**
Fuel gas pressure	**0.25~0.45(MPa)**
Carrier gas pressure	**0.1(MPa)**
Spray distance	**70(mm)**
Traverse speed of gun	**8.3×10^{-2}(mm/s)**
Step width	**4.0(mm)**
Nozzle length	**100,130(mm)**

(70%C_2H_2+30%C_3H_6) (Wellcat) and the powder carrier gas was nitrogen. The HVOF system is preferred over the plasma system, because of the lower mean particle temperature and shorter residence time, which diminishes the tendency for transformation into high temperature microstructure [9] (from anatase to rutile).

Table 2 shows conditions of HVOF spraying. The fuel gas pressure has been changed from 0.25 to 0.45MPa in the present study.

SUS304 steel (50mm×60mm×3mm) substrates were used for thermal spraying.

By collecting particles using carbon adhesive tape before reaching the substrate, the transformation behavior could be studied in detail. **Fig.3** shows a schematic illustration of collecting sprayed (flying) particles.

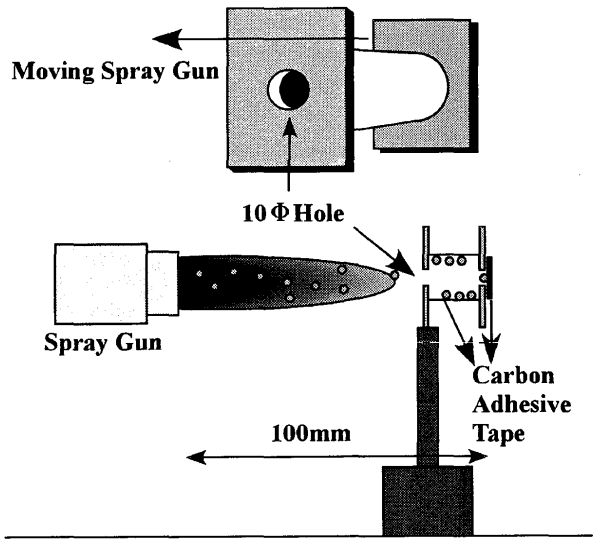

Fig.3 Schematic illustration for collecting spraying (flying) Particles by using carbon tape.

3. Results and discussion

3.1 Microstructure of the coating (The influence of arc current on the formation of coating)

The heat input into particles was adjusted by changing arc current in the plasma spray. **Fig.4** shows surface morphologies and cross-sectional images of P_{200} TiO_2 coating sprayed using P_{200} powders. It is possible to achieve approximately 100 μm thickness on the substrate at 800A, while the thickness of the TiO_2 coating was drastically decreased at 400A and the area fraction of porosity in the coating was higher. **Fig.5** shows X-ray diffraction patterns of the coatings sprayed with P_{200} powders. X-ray peaks due to anatase (101) were narrowly detected at all arc currents. The rutile phase was dominant in the coating when plasma spray was conducted.

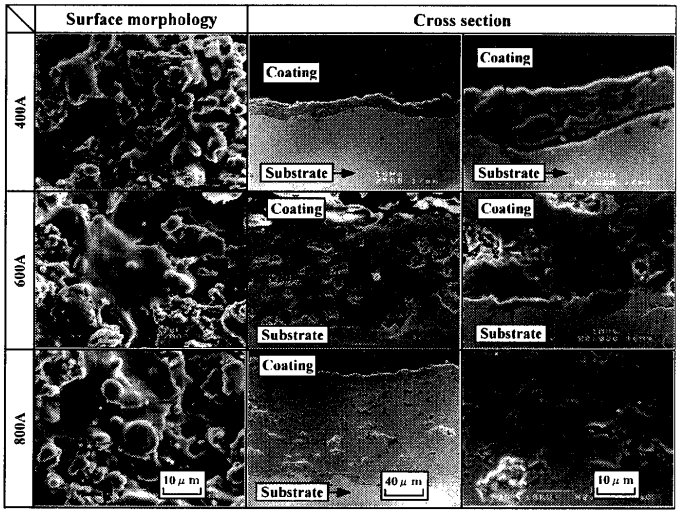

Fig.4 Surface morphologies and cross sections of sprayed P_{200} coatings at various arc currents.

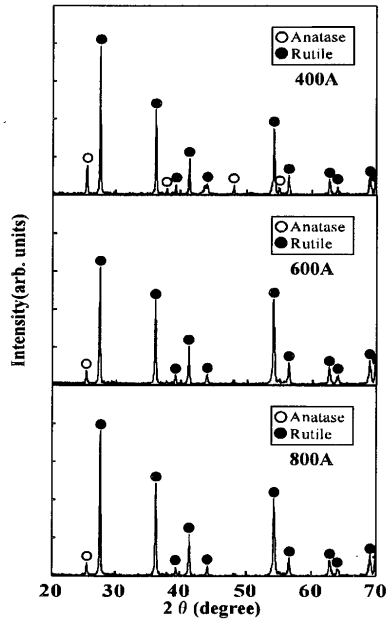

Fig.5 X-ray diffraction patterns of sprayed P_{200} coatings at various arc currents.

Fig.6 shows the relation between anatase ratio and arc current. The anatase ratio was estimated by using equation (1). The anatase ratio of coatings was lower and coating thickness was increased with increased of arc current as shown in Fig.5.

The plasma flame temperature was lower with decreasing arc current and therefore powder heating is suppressed. Surface morphology showed this phenomenon, which could be observed as fine white particles on the surface at 400A and exhibited continuous non-bonded lines between topcoat and substrate.

It can been seen that the area fraction of porosity (non-bonded area) in the TiO_2 coating was observed at lower arc current (400A) because there were few traces of melted particle by comparision with higher currents (600A, 800A). It was seen that the TiO_2 coating was formed by a short-time solid bond process. The melting particles are necessary to get a well-bonded coating, however the higher fraction of anatase phase in TiO_2 coatings is essential to show high active photo-catalytic property. Consequently, a high anatase ratio and well-bonded thick coating without porosity are not compatible with each other in the case of plasma spray process.

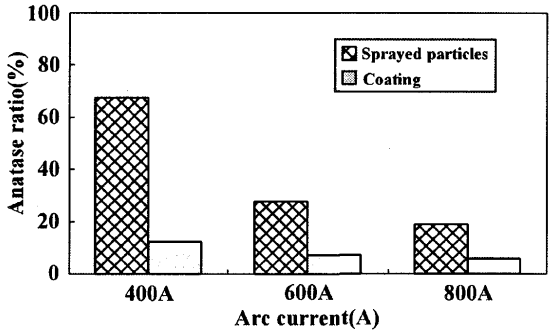

Fig.6 Anatase ratio in spraying P_{200} particles and coating at various arc currents.

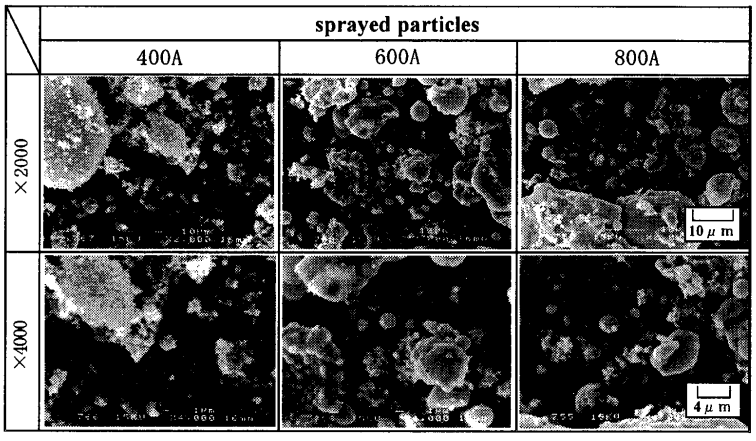

Fig.7 SEM micrographs of sprayed P_{200} particles collected on the tape at various arc currents.

It is necessary to catch flying TiO_2 particles before reaching the substrate in order to investigate melting and transfomation behavior.

Fig.6 also shows the anatase ratio in both spraying (flying) P_{200} particles and coatings at various arc currents.

There is a big difference in anatase ratio between flying particle and formed coatings although the anatase ratio of collected particle increased with decreasing arc current as well as coating. It was found that almost all transformation from anatase into rutile phase occurred on substrates. The substrate has a tendency to accumulate heat and to increase in temperature above 1188K during plasma spraying because it is difficult to disperse heat from the 304 austenitic stainless substrate. Both plasma flame and substrate provide heat for deposited particles just after impacting onto the substrate. In the case of 400A arc current, the difference of anatase ratio between collected particles and the coatings was biggest.

The anatase type particles transform into rutile phase above 1188K at shorter times. This biggest difference between flying particles and coating at 400A seems to become representative of a multiplier effect, i.e. the heating from both substrate and plasma flame during spraying easily causes the transformation.

However, Fig.6 shows that the heating just after impact is mainly affected although the plasma arc directly contributed to increase of particle temperature during flying.

Fig.7 shows SEM micrographs of sprayed P_{200} particles collected on the tape before reaching on substrate. It can be observed that agglomerated particles did not disperse in the plasma jet and kept their primary particle shape at 400A.

TiO_2 particles less than 1μm diameter were observed at 600A and 800A in some areas and the primary shape was not found. These fine particles were little observed in the coating. Fine non-melted particles retain their anatase phase during flying, but almost all anatase fine particles will transform on the substrate.

Fig.8 shows surface morphologies and cross sections of plasma sprayed coatings using P_{30} powders. The coating thickness also increased with increasing arc current when P_{30} powders were used as well as P_{200} powders. However the anatase ratio was greatly decreased by changing particle size, which was approximately 5% at every current step as shown in **Fig.9**.

Fine TiO_2 particles were observed on the coating surface at low arc current (400A) and the roughness become greater with decreasing arc current when plasma spraying was applied. By using P_{30} powders, relatively thinner coatings were produced as compared to P_{200} powder.

The mobility of powder into the plasma jet was not great enough during spraying because nano-powders have not sufficient gravity, thus it seemed that there are differences in coating thickness.

It is asummed that nano-size particles easily transform into rutile phase even if the powder is subjected to the same heat input (similar temperature) and thermal conductivity will become higher than that of sub-micron size TiO_2 powders. However such kinds of phenomenon were not observed, so it can be supposed that dispersed fine 30nm particles, by impacting on the substrate, drastically transform on or near the substrate.

Fig.9 also suggests that nano-particles (30nm) give rise to the possibility of decreasing transformation temperature. The anatase ratio in flying of P_{30} particles and the coating are also shown in Fig.9. As well as for the P_{200} powders, the anatase ratio of collected particles was higher at every current, however, there is little difference at 600A and 800A for P_{30} powders. The difference at 400A was notable because nano-particle and higher anatase ratio can be acquired by plasma spray. The flying particles were collected by using carbon tape in order to investigate this difference.

Fig.10 shows SEM micrographs of sprayed P_{30} particles collected on the tape at various arc currents. It is clear that non-destroyed (non-dispersed) agglomerated powder can be observed at 400A.

Once agglomerated particles (33.3μm) divide into individual fine particle (30nm), nano-particle will transform in short times during flying because the real contact (surface) area with high temperature will be drastically increased. Since the agglomerated powders are kept primarily spherical-shape at 400A before reaching

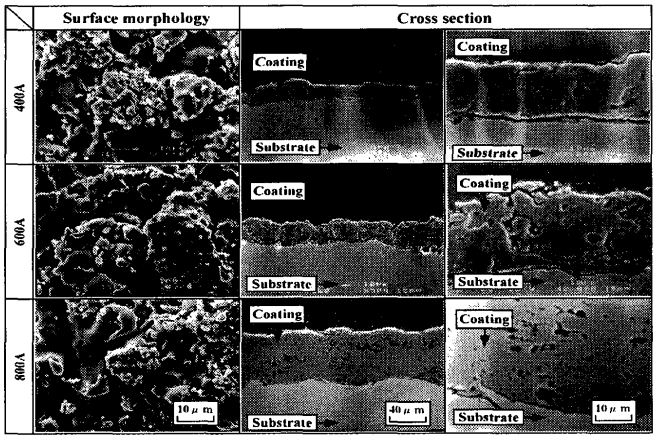

Fig.8 Surface morphologies and cross-sectional images of coating sprayed by P_{30} powder at various arc current.

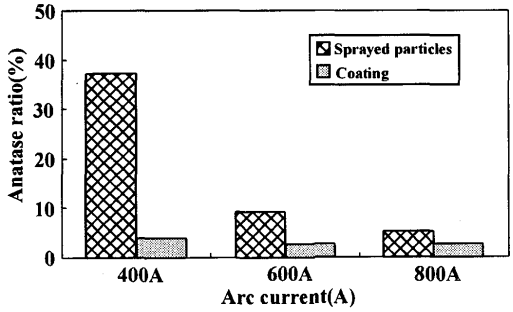

Fig.9 Anatase ratio in sprayed P_{30} particles and coating.

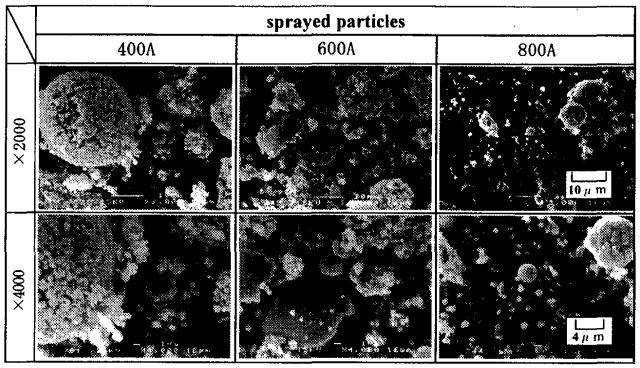

Fig.10 SEM micrographs of sprayed P_{30} particles collected on the tape at various arc currents .

substrate, the real contact (surface) area with high temperature will be drastically decreased and consequently a higher anatase phase remains as compared to higher arc current.

3.2 Microstructure of coatings by High Velocity Oxy-Fuel (HVOF)

Fig.11 shows surface morphologies and cross sectional-images of sprayed P_{200} coatings with Cu undercoat at various fuel gas pressures. The trace of melted-particle similar to splat phenomenon was seen in case of plasma spray at higher arc current, however, such behavior was not observed in High Velocity Oxy-fuel (HVOF). The coating thickness was increased with increasing fuel gas pressure. It can be seen that fine particles were piled up on the substrate.

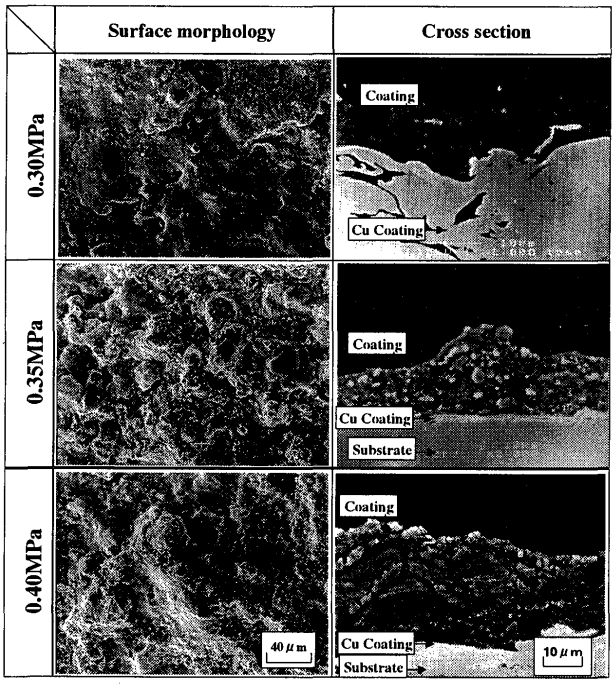

Fig.11 Surface morphologies and cross sectional-images of sprayed P_{200} coating with Cu undercoating at various fuel gas pressures.

In particular, the obvious continuous non-bonded line has been observed at 0.4MPa fuel gas pressure.

Fig.12 shows X-ray diffraction patterns of sprayed P_{200} coatings. The X-ray peak of the Cu undercoat was detected because of non-uniform thickness.
The anatase X-ray peak was strongly detected in contrast with plasma sprayed coatings although Cu peak was detected.

Fig.13 shows the anatase ratio in sprayed P_{200} coatings at various fuel gas pressure. The HVOF system can provide approximately 80% anatase ratio at the lowest gas pressure and it was possible to maintain 50% anatase ratio by raising gas pressure (up to 0.40MPa). High particle speeds enable TiO_2 particles to produce coatings even for lower temperatures. According to microstructure, the adhesion strength between particles was not good. It will be necessary to bond individual particles better to

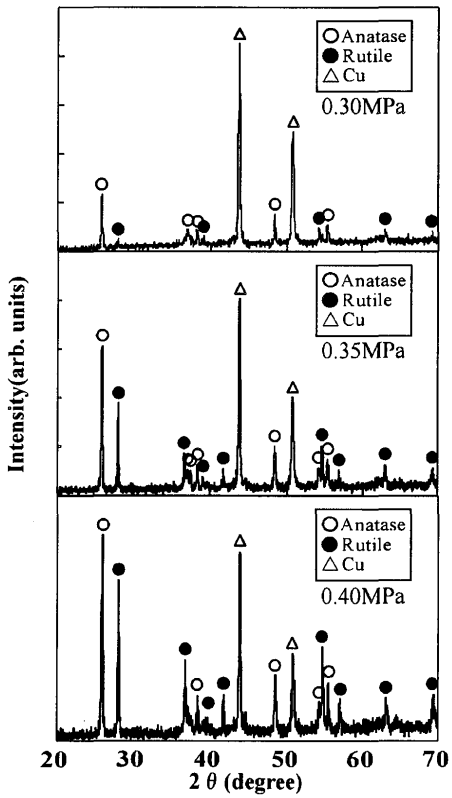

Fig.12 X-ray diffraction patterns of sprayed P_{200} coatings.

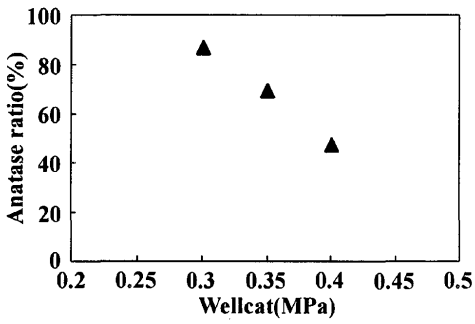

Fig.13 Anatase ratio in sprayed P_{200} coatings at various fuel gas pressures.

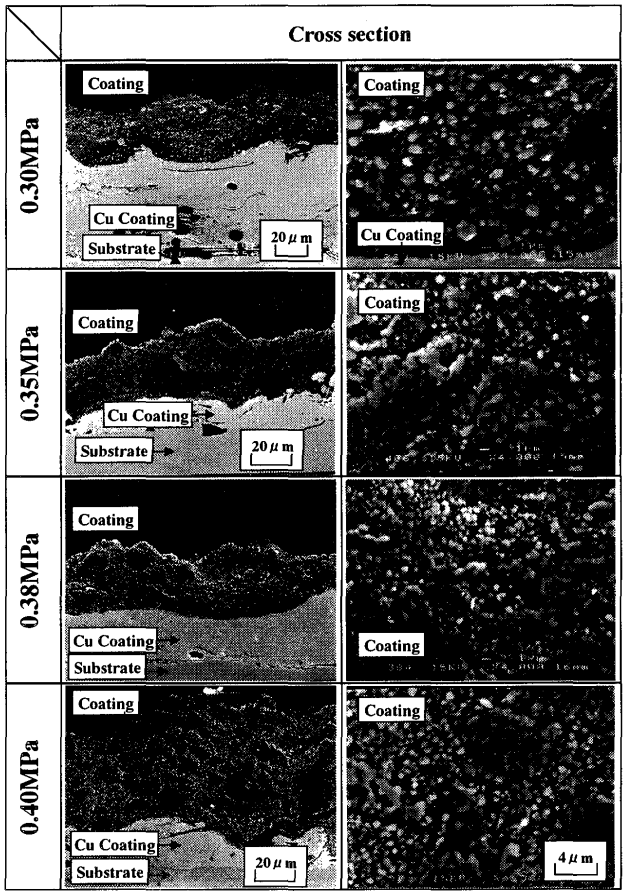

Fig.14 The cross-sectional images of sprayed P_{30} coatings at various fuel gas pressures.

produce uniform coatings.

Fig.14 shows cross-sectional images of the sprayed P_{30} coatings at various fuel gas pressures. There are observations of large crevices in the coatings and the white fine particles were dispersed uniformly on the coating surface. According to observation of cross-sectional images, it can be expected that flying particles were bonded tightly into the substrate in the as-sprayed condition and then were formed without melting up to high temperatures.

The coating thickness is approximately 50~60 μm even if adhesion strength seems to be not enough and it was possible to accumulate on the substrate.

Fig.15 shows X-ray diffraction patterns of sprayed P_{30} coatings. X-ray peaks from the Cu undercoat were also detected because of non-uniform coated thickness.

The anatase X-ray peak was strongly detected as well as in the P_{200} coating and the Cu peak was also detected. Peak height at the anatase phase has increased with decreasing fuel gas pressures.

The anatase peak is strongly detected relatively to the rutile peak at lower pressures although thickness is decreased.

Fig.16 shows the anatase ratio in sprayed P_{30} coatings at various fuel gas pressures. It was possible to obtain approximately 80% anatase ratio at the lowest gas pressure (0.3MPa) and it was possible to maintain 50% anatase ratio by raising the gas pressure (up to 0.40MPa). This kind of phenomenon is similar to the tendency in P_{200} coatings.

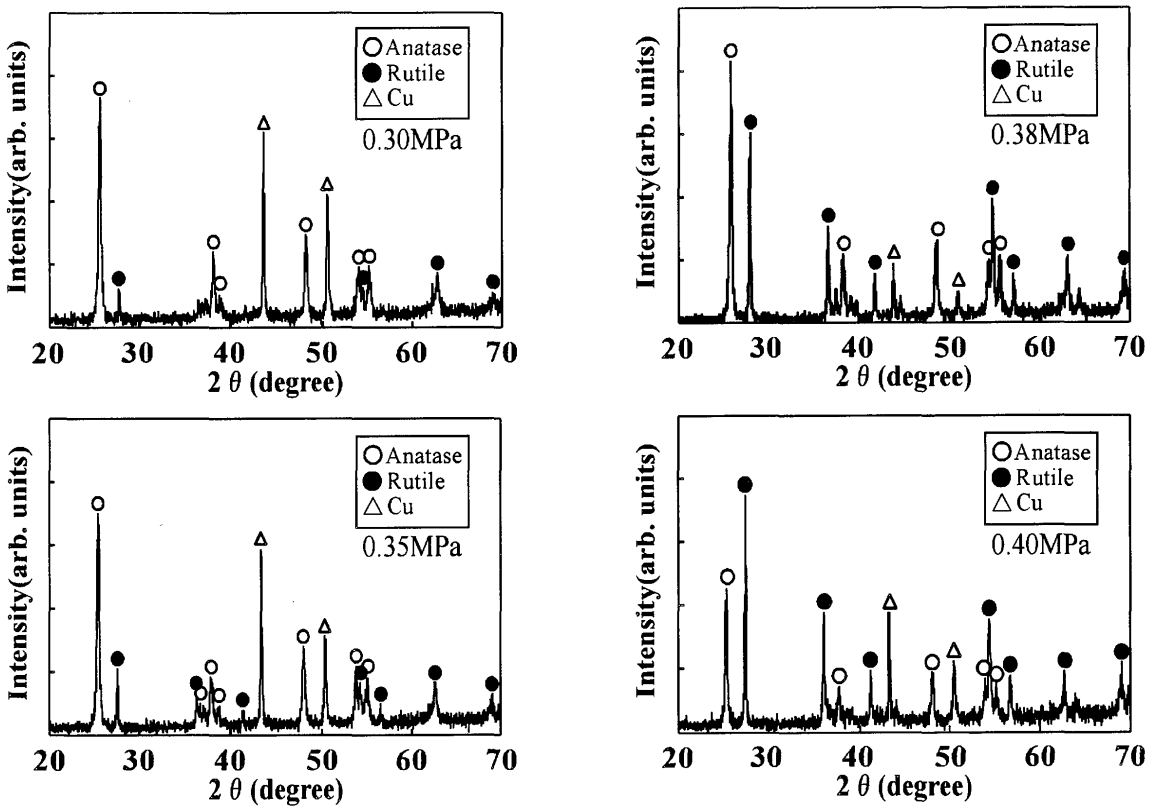

Fig.15 X-ray diffraction patterns of sprayed P_{30} coatings.

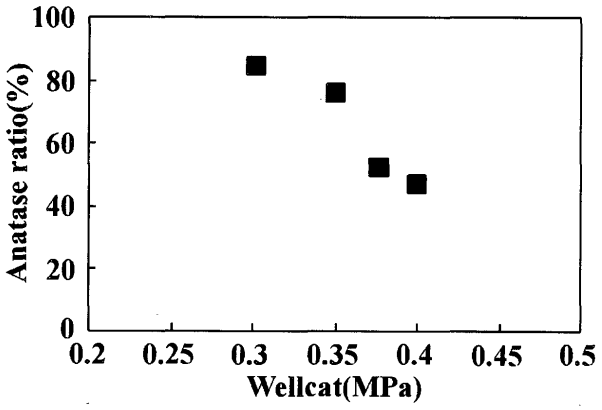

Fig.16 Anatase ratio in sprayed P_{30} coatings at various fuel gas pressures.

The HVOF process can provide both lower flame temperature and high velocity, and consequently can drastically suppress transformation into rutile. These high velocity enables TiO_2 particles to form the coatings even at lower temperature.

The coating was formed by accumulating TiO_2 particle having diameter of 30μm~40μm on substrate without loosing their primary shape when HVOF was used, while a high fraction of crevices (porosity) could be observed when plasma spray was used.

HVOF is recommended to provide a high fraction of anatase phase, but, the sprayed TiO_2 coating itself was not stable because of non-melted areas. The approximately 80% anatase ratio will be enough for photo-catalytic because thermal spray technique can provide coating over the highest area, however there are possibilities of exfoliation and falling away of particles during application. On the other hand, it is necessary to adopt plasma spray to achieve stable coatings. Both a high fraction of anatase and stable coatings were not compatible in the present investigation.

4. Conclusions

1) TiO_2 coating was deposited on stainless steel by plasma spraying and the HVOF process. The coating having a high fraction of anatase was developed by HVOF process, while the anatase ratio drastically decreased in plasma spraying.

2) Plasma spraying can provide a uniform coating in contrast to HVOF since coating is formed by a melting process.
TiO_2 particle flying in the plasma jet showed higher anatase ratio than that of TiO_2 coating at all currents.

3) The possibility of thermal sprayed coating has been demonstrated because 80% anatase ratios can been achieved when nanostructure of 30nm particles were used by HVOF process.

References

1) Iis Sopyan , Mitsuru Watanabe , Sadao Murasawa, Kazuhiko Hashimoto, Akira Fujishima, An efficient TiO_2 thin-film photocatalyst : photocatalytic properties in gas-phase acetaldehyde degradation, Journal of Photochemistry and Photobiology A : Chemistry 98 (1996) 79-86.

2) Eva-Maria Bonsen , Stefan Schroeter , Hervert Jacobs , Jose A.C. Broekaert , PHOTOCATALYTIC DEGRADATION OF AMMONIA WITH TiO_2 AS PHOTOCATALYST IN THE LABORATORY AND UNDER THE USE OF SOLAR RADIATION, Chemosphere, 1997 , Vol.35 , No.7 , pp1431-1445.

3) Darrin S.Muggli , Lefei Ding , Photocatalytic performance of sulfated TiO_2 and Degussa P-25 TiO_2 during oxidation of organics , Applied Catalysis B : Environmental 32 (2001) 181-194.

4) Jiangyan Qin , Ken-ichi Aika , Catalytic wet air oxidation of ammonia over alumina supported metals, Applied Catalysis B: Emvironmental 16 (1998) 261-268.

5) M.Muneer,J.Theurich,D.Bahnemann,Titaniumdioxide mediated photocatalytic of degradation 1,2-diethyl phthalate", Journal of Photochemistry and Photobiology A:Chemistry 143(2001) 213-219.

6) M.Dj. Blesic, Z.V. Saponjic, J.M. Nedeljkovic, D.P. Uskokovic, TiO_2 films prepared by ultrasonic spray pyrolysis of nanosize precursor, Materials Letters 54 (2002) 298-302.

7) M.L. Lau, V.V. Gupta and E.J. Lavernia , PARTICLE BEHAVIOR OF NANO-CRYSTALLINE 316-STAINLESS DURING HIGH VELOCITY OXY-FUEL THERMAL SPRAY, NanoStructured Materials , 1999 , Vol.12 , pp.319-322.

8) Robert A. Spurr and Howard Myers, Quantitative Analysis of Anatase-Rutile Mixtures with an X-ray Diffractometer, Analytical Chemistry, Vol.29, No.5 , (1957) , 760-762.

9) A.W.Czanderna, C.N.Rmachandra Rao and J.M.Honig, "The anatase-rutile transition", Trans.Faraday Society (1958) 1069-1073.